Dynamics of Cellular Patterns

James A. Glazier†

Research Institute of Electrical Communication Tohoku University, 2-1-1 Katahira, Sendai 980, JAPAN

Many materials are cellular: polycrystalline metals, soap froths, lipid monolayers, geographical territories, convective cells, magnetic bubbles and biological tissues, among others.¹, ²

How can we characterize cellular patterns? We consider 2-d patterns because we understand them better. They are composed of compact polygonal cells (or grains, domains, bubbles, etc...), which are separated from each other by a continuous network of narrow boundaries. Generally the boundaries meet at three-fold vertices at approximately 120° angles. Boundaries are usually close to minimal surfaces. These properties arise from surface tension or energy minimization.³

Beginning with the work of C. Smith in the early 1950's, the soap froth has been the prototype for all cellular patterns which coarsen in time by losing cells.⁴ Cell growth and disappearance are caused by surface energy driven diffusion, and obey the simple law derived by von Neumann for polygonal cells:⁵

$$\frac{\mathrm{da}}{\mathrm{dt}} = \kappa'(n - 6) , \qquad (1)$$

where κ' is a diffusion constant and n the number of sides of a cell. Since the rate is independent of area, at long times the average area per cell <a> ∞ t. Rounded cells obey the Lifschitz-Slyozov law:

$$\frac{\mathrm{da}(\mathbf{r})}{\mathrm{dt}} = \kappa' \left(\left\langle \frac{1}{\mathbf{r}} \right\rangle - \frac{1}{\mathbf{r}} \right),\tag{2}$$

leading to $\langle a \rangle \propto t^{2/3}$. Unfortunately there is no equivalent to von Neumann's law in 3-d.

Besides the local von Neumann's law, topological processes, e.g. cell disappearance, affect the number of sides and evolution of several cells. We characterize cellular patterns by their distribution functions, e.g. $\rho(n)$, the probability that a cell has n sides, and their correlation functions. We find empirically that patterns reach a scaling state, in which these remain constant, and only <a> increases (fig. 1 (a)).7

There are many types of simulations, including simple mean field theories, topological network models, vertex models,

boundary dynamics models, and the Potts model. Several can duplicate both the transient and the scaling state. However, a mathematical physicist recently commented "As far as I can see, we do not have a theory of bubbles. We do have a large collection of 'recipes,' we do have a large collection of data and empirics; but not a theory."8

In the Potts model, the pattern is subdivided into a regular lattice, with each cell assigned an unique 'spin' identification, σ . A cell, σ , is the collection of lattice sites, (i,j), with spin, $\sigma(i,j)=\sigma$. The energy is the boundary length, i.e., the number of neighboring sites in the lattice with different spins:

$$H_{\text{Potts}} = \sum_{(i,j)(i',j') \text{ neighbors}} 1 - \delta_{\sigma(i,j),\sigma(i',j')}$$
(3)

At each time step a site and trial spin are selected at random. Substitutions are made with probability, P={1, $\Delta H < 0$; $e^{-\Delta H/T}$, $\Delta H \leq 0$ }, where ΔH is the change in H_{Potts} . Using a soap froth image as the initial condition, we find that the statistical evolution of the model agrees with the experiment.¹⁰

The anisotropy of the lattice makes a quantitative difference to the distributions, and at low temperatures or high anisotropies can cause the simulation to freeze. However, in the low anisotropy limit we recover the soap froth results.

At the level of simulations we now understand the 'ideal coarsening' of soap. We understand somewhat the effects of anisotropy, defects and pinning centers which are common in metals. Two complex systems have been studied fairly extensively: lipid monolayers and magnetic domains.

Lipid monolayers consist of an amphiphilic lipid floated on a water surface. Depending on temperature and pressure there is a transition from a two dimensional 'gas' phase to a 'liquid' phase. Because the two phases are composed of the same material, their volume fraction can be varied between a close packed and a round cell limit. Experimental observations suggest that the former obeys von Neumann statistics and the latter Lifschitz-Slyozov. The intermediate regime is not well understood, and so far no one has attempted to model it.

Magnetic domains are more complex, since besides their surface energies there is a long range dipole interaction between cells. In addition the boundaries between cells are not single walls but double, and repel each other, stabilizing small cells at a characteristic size (fig. 1 (b)). The pattern therefore evolves not in time but in the applied magnetic field. We can expand the energy in in powers of the areas, $a(\sigma)$, beginning: 13

$$H_{\text{Mag}} = \sum_{(i,j)(i',j')}^{\text{neighbors}} J(1 - \delta_{\sigma(i,j),\sigma(i',j')}) + \lambda \sum_{\text{spins s}} (a(\sigma) - A_{\sigma})^2 + ..., \quad (4)$$

where A_{σ} is the target area set by the competition between the wall energy and the bulk area energy. There is no scaling state, nor power law area growth. Above a critical field five-sided cells collapse causing a catastrophic increase in length scale.

Soap bubbles have long been used as models for tissues. ¹⁴ In embryology, it remains an open question how cells move where they need to go. How does the liver separate from the heart, for instance? Embryos can resort if they are artificially mixed. ¹⁵ Such ability is reduced in adults, but occurs in wound healing, where cells migrate to reform ablated tissue. ¹⁶ The adult *hydra* can be dissociated into randomly mixed single cells, be formed into a lump, yet reorganize into a normal animal. ¹⁷

Cell sorting is associated with the presence of several cell type specific surface molecules, e.g. cadherins, affect cell-cell contact energies. ^{15, 18} To study cell sorting we we include a cell type, $\tau(\sigma)$ in our energy. The target area, A_{τ} , and the energy per unit of boundary, $J(\tau,\tau')$, then become functions of τ , yielding: ¹⁹

$$\begin{split} H_{Sort} = & \sum_{(i,j)(i',j')}^{neighbors} J(\tau(\sigma(i,j)),\tau(\sigma(i',j')))(1-\delta_{\sigma(i,j)},\sigma(i',j')) + \\ & \lambda \sum_{spin\ types\ \sigma} \left(a(\sigma)-A_{\tau(\sigma)}\right)^{2}. \end{split} \tag{5}$$

There are a number of problems choosing the parameters, temperature, etc... for this simulation.²⁰ However, if take the heterotypic interface energy between the homotypic interface energies, we obtain classical cell sorting (fig. 2), including the sorting of the surface before the bulk. If we vary the relative energies and initial conditions, we obtain such biological phenomena as engulfment, cell mixing, partial cell sorting, reversed cell sorting and dissociation (fig. 3). Most simulations exhibit logarithmic time dependence, suggesting that temperature driven fluctuations are important.

Thus we are able to explore several extensions to ideal grain growth of soap froth. We are able to simulate using a variety of methods, though we do not have any analytic theory. We are beginning to study biological cells, which may give insight into embryological development.

- † Permanent address: Department of Physics, University of Notre Dame, Notre Dame, IN 46556, USA.
- ¹ D. Weaire and N. Rivier, *Contemp. Phys.* **25**, 59 (1984). (review article).
- ² J. A. Glazier and D. Weaire, *J. Phys.: Condens. Matter* **4**, 1867 (1992) (review article).
- ³ J. A. Glazier, *The Evolution of Cellular Patterns*, Ph.D. dissertation, University of Chicago, 1989.
- ⁴ C. S. Smith, *Metal Interfaces*, Cleveland: American Society for Metals, 65 (1952).
- ⁵ J. von Neumann, *Metal Interfaces*, Cleveland: American Society for Metals, 108 (1952).
- ⁶ I. M. Lifschitz and V. V. Slyozov, *Soviet JETP* **35**, 331 (1959). and *J. Phys. Chem. Solids* **19**, 35 (1961).
- ⁷ J. A. Glazier, S. P. Gross, and J. Stavans, *Phys. Rev. A.* **36**, 306 (1987).
 - ⁸ M. Magnasco, unpublished (1992).
- ⁹ D. J. Srolovitz, M. P. Anderson, P. S. Sahni, and G. S. Grest, *Acta Metall.* **32**, 793 (1984).
- 10 J. A. Glazier, M. P. Anderson, and G. S. Grest, *Phil. Mag. B* 62, 615 (1990).
- ¹¹ E. Holm, J. A. Glazier, D. J. Srolovitz, and G. S. Grest, *Phys. Rev. A* **43**, 2662 (1991).
- ¹² K. J. Stine, S. A. Rauseo, B. G. Moore, J. A. Wise, and C. M. Knobler, *Phys. Rev. A* **41**, 6884 (1990). B. Berge, A. J. Simon, and A. Libchaber, *Phys. Rev A* **41**, 6893 (1990).
- 13 D. Weaire, F. Bolton, P. Molho, and J. A. Glazier, J. Phys. Condens. Matter 3, 2101 (1991).
- ¹⁴ D'A. W. Thompson, *On Growth and Form*, 2nd edition, Cambridge University Press (1942). F. T. Lewis, *Anat. Rec.* **38**, 341 (1928). E. B. Matzke, *Proc. Natl. Acad. Sci. (USA)* **31**, 281 (1945).
- ¹⁵ P. Armstrong, *Crit. Rev. Biochem. and Mol. Biol.* **24**, 119 (1989) (review article).
 - ¹⁶ R-M. Mège, médecines/sciences 7, 544 (1991) (in French).
 - ¹⁷ K. Noda, *Zool. Mag.* **80**, 99 (1971) (in Japanese).
 - 18 F. Graner and Y. Sawada, preprint (1992).
 - ¹⁹ F. Graner and J. A. Glazier, *Phys. Rev. Lett.* to appear (1992).
 - ²⁰ J. A. Glazier and F. Graner, preprint (1992).

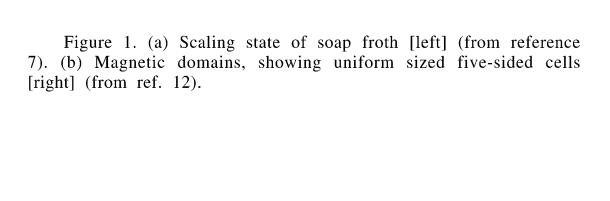


Figure 2. Cell sorting simulation. (a) Partially sorted state [left]. (b) Totally sorted state [right] (from ref. 19).

Figure 3. Cell sorting simulation. (a) Cell mixing [left]. (b) Partial cell sorting [right] (from ref. 20).